

A single-molecular magnet: $[\text{Mn}_{12}\text{O}_{12}(\text{O}_2\text{CCH}_2\text{Br})_{16}(\text{H}_2\text{O})_4]$

Hui-Lien Tsai^{a,*}, Da-Min Chen^a, Chen-I Yang^a, Tyn-Yih Jwo^a, Ching-Shuei Wur^b,
Gene-Hsiang Lee^c, Yu Wang^c

^a Department of Chemistry, National Cheng Kung University, Tainan, Taiwan, ROC

^b Department of Physics, National Cheng Kung University, Tainan, Taiwan, ROC

^c Instrumentation Center, College of Science, National Taiwan University, Taipei, Taiwan, ROC

Received 15 March 2001; accepted 12 June 2001

Abstract

The synthesis, X-ray crystal structure and magnetic properties of a new dodecanuclear manganese complex $[\text{Mn}_{12}\text{O}_{12}(\text{O}_2\text{CCH}_2\text{Br})_{16}(\text{H}_2\text{O})_4] \cdot 4\text{CH}_2\text{Cl}_2(\mathbf{2}) \cdot 4\text{CH}_2\text{Cl}_2$ are reported. Complex $\mathbf{2} \cdot 4\text{CH}_2\text{Cl}_2$ crystallizes in tetragonal space group $I4_1/a$ with the following cell dimensions at 293(2) K: $a = b = 26.697(4)$ Å, $c = 13.246(4)$ Å, and $Z = 4$. The results of DC and AC magnetic susceptibility studies are described. DC measurements show the presence of hysteresis loops, and the out-of-phase component of AC magnetic susceptibilities has a frequency dependent maximum. Step-like features are seen on hysteresis loops and quantum mechanical tunneling could be the origin of these unusual relaxations. © 2001 Published by Elsevier Science B.V.

Keywords: Crystal structure; Single-molecule magnet; Step-like hysteresis loop; Magnetic quantum tunneling

1. Introduction

Single-molecule magnets (SMM) are attracting extensive attention because they represent nanoscale magnetic particles of a well-defined size [1–16]. They display sluggish magnetization relaxation phenomena such as magnetization hysteresis loops and frequency-dependent out-of-phase alternating current (AC) magnetic susceptibility. The remarkable magnetic properties of an SMM arise from the SMMs high-spin ground state (S) split by a large negative axial zero-field splitting (D) which results in an anisotropy energy barrier of $KV = |D|S_z^2$ [17,18]. The first SMM reported was $[\text{Mn}_{12}\text{O}_{12}(\text{O}_2\text{CCH}_3)_{16}(\text{H}_2\text{O})_4] \cdot 2\text{HOAc} \cdot 4\text{H}_2\text{O}$ ($\mathbf{1}$) with $S = 10$ ground state and a negative zero-field splitting of -0.5 cm⁻¹ [1–5,8–11]. We herein describe the preparation, X-ray structure and magnetic properties of a new SMM, $[\text{Mn}_{12}\text{O}_{12}(\text{O}_2\text{CCH}_2\text{Br})_{16}(\text{H}_2\text{O})_4] \cdot 4\text{CH}_2\text{Cl}_2(\mathbf{2}) \cdot 4\text{CH}_2\text{Cl}_2$.

2. Experimental

2.1. Synthesis

A slurry of complex $\mathbf{1}$ (0.25 g, 0.125 mmol) [19] in toluene (6.5 ml) was treated with an excess of the $\text{HO}_2\text{CCH}_2\text{Br}$ (0.476 g, 3.43 mmol). The mixture was concentrated to remove acetic acid as the toluene azeotrope. As the solvent volume was reduced, the black solid slowly dissolved. When almost all the toluene had been removed, more toluene (6.5 ml) was added and removed by evaporation, and the process repeated twice. The resulting oil was dissolved in toluene, and treated with a further amount of $\text{HO}_2\text{CCH}_2\text{Br}$ (3.41 mmol) and the entire process repeated. After the final evaporation, the resulting oil was dissolved in CH_2Cl_2 (20 ml), and filtered to remove any undissolved solid. The resulting filtrate was layered with hexanes (50 ml), stored at room temperature for several days and afforded suitable crystals for the X-ray crystal structure analysis. The resultant black crystals were collected by filtration, washed copiously with hexanes and dried in vacuo. The overall yield of $\mathbf{2}$ was ~84%. Elemental analysis calculated for $[\text{Mn}_{12}\text{O}_{12}(\text{O}_2\text{CCH}_2\text{Br})_{16}(\text{H}_2\text{O})_4] (\mathbf{2})$, $\text{C}_{32}\text{H}_{40}\text{Br}_{16}\text{Mn}_{12}\text{O}_{48}$: C 12.28, H 1.29, Mn 21.06; found: C 12.16, H 1.35, Mn 20.96%.

* Corresponding author. Tel.: +886-6-275-7575; fax: +886-6-274-0552.

E-mail address: hltsai@mail.ncku.edu.tw (H.-L. Tsai).

2.2. Crystallography

Crystal data of complex **2** · 4CH₂Cl₂: C₃₆H₄₈Br₁₆Cl₈Mn₁₂O₄₈, $M = 3470.18$, black plate, crystal dimensions $0.40 \times 0.40 \times 0.20$ mm, tetragonal, space group $I4_1/a$, $a = b = 26.697(4)$ Å, $c = 13.246(3)$ Å, $V = 9441(3)$ Å³, $Z = 4$, $D_{\text{cal}} = 2.441$ g cm⁻³, $F(000) = 6576$, $\mu(\text{Mo-K}\alpha) = 8.629$ mm⁻¹. Determination of cell constants and data collections were carried out on an Nonius CAD4 diffractometer using an ω - 2θ scan mode in the range $1.53 \leq \theta \leq 25.00^\circ$ with graphite monochromated Mo-K α radiation ($\lambda = 0.71073$ Å) at 293(2) K. A total of 4154 unique reflections were collected. Crystal decay was monitored every 60 min and 8% decay was observed. An empirical absorption from PSI-can was applied. The structure was solved using the direct method in SHELXS 97 [20] and refined with all non-hydrogen atoms anisotropic except C8 by full-matrix least-squares on F^2 (SHELXL 97 [21]). Refinement converged at $R1 = 0.0883$ and $wR2 = 0.1764$ for 4154 unique data [$I > 2\sigma(I)$], goodness-of-fit = 1.030, where $R1 = \sum ||F_o| - |F_c|| / \sum |F_o|$; $wR2 = \{ \sum [w(F_o^2 - F_c^2)^2] / \sum [w(F_o^2)^2] \}^{1/2}$, and weight scheme $w = [\sigma^2(F_o^2) + (0.0655P)^2]$, where $P = (F_o^2 + 2F_c^2)/3$. Maximum and minimum peaks in the final difference map were 1.056 and -1.504 eÅ⁻³.

2.3. Magnetic measurements

A polycrystalline of complex **2** was suspended in eicosane at 313 K, oriented in a 7.0 T field and then the eicosane matrix was cooled to room temperature. This gives a waxy cube with the crystals aligned with their easy axes of magnetization parallel. Magnetization hysteresis data were measured by a SQUID magnetometer (Quantum Design, MPMS-7). The oriented polycrystalline sample of complex **2** was saturated in a field of +3.0 T then swept down to -3.0 T, and cycled back to +3.0 T at ten different temperatures between 1.7 and 2.6 K. Alternating current susceptibility measurements were carried out on a quantum design PPMS-9 magnetometer equipped with a 9.0 T magnet. One set of AC susceptibility data was collected for powdered, microcrystalline sample in an AC field of 1.0 Oe, oscillating in the 250–10 000 Hz range.

3. Results and discussion

3.1. Structure

The structure of the complex **2** is shown in Fig. 1. The structure of complex **2** is quite similar in many respects to complex **1** [19]. Complex **2** is in $\bar{4}$ symmetry which possesses a [Mn₁₂(μ_3 -O)₁₂] core having a central [Mn₄^{IV}O₄]⁸⁺ cubane held within a nonplanar ring of eight

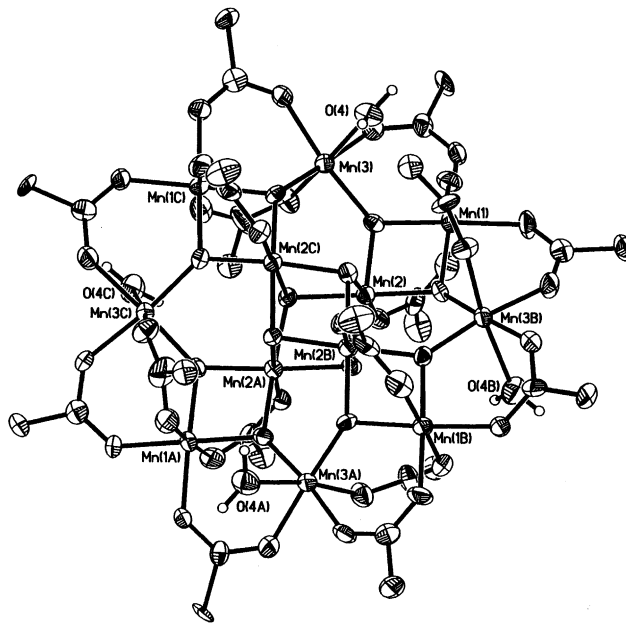


Fig. 1. The X-ray structure of complex **2** at the 30% probability level. The $-\text{H}_2\text{Br}$ groups of the ligands, and CH_2Cl_2 solvate molecules are omitted for clarity.

Mn^{III} ions by eight μ_3 -O²⁻ ions. Peripheral ligation of complex **2** is proved by sixteen η^2 - μ_2 -carboxylate groups and four H₂O ligands. Complex **2** has one H₂O ligand on each Mn^{III} ion in one set of four Mn^{III} ions which are bonded to two Mn^{IV} ions via two μ_3 -O²⁻ ions. The Mn–O bond distances make it clear that all of the atoms in the central cubane are Mn^{IV} ions, while the ring consists of eight Mn^{III} ions. These assignments supported by the marked Jahn–Teller elongation of the axial Mn^{III}–O bonds (2.10–2.22 Å), which are on average 0.24 Å longer than the analogous equatorial Mn–O bonds (1.86–1.96 Å).

3.2. Magnetochemistry

The data of hysteresis loops at ten temperatures are shown in Fig. 2. Steps are clearly seen on these hysteresis loops, as was reported for complex **1** [22,23]. In Fig. 3 is shown the first derivative of the hysteresis plots. As the field is decreased from +3.0 T, the first step is seen at zero field, followed by steps at -0.4546 , -0.9154 , -1.3163 , -1.7970 and -2.2178 T. Such steps in a hysteresis loop have been shown to be due to increases in the rate of change of the magnetization, and are correspond to resonant tunneling between quantum spin states. The spacing between the steps in the hysteresis loops is given as $\Delta H = -D/g\mu_B$, where g is the gyromagnetic factor and μ_B is the Bohr magneton. The parameter D is the magnitude of axial zero-field splitting ($|D|S_z^2$). From Fig. 3, we calculate the average step size to be $\Delta H = 0.45$ T, which is similar to the value $\Delta H = 0.44$ T obtained for **1** [2].

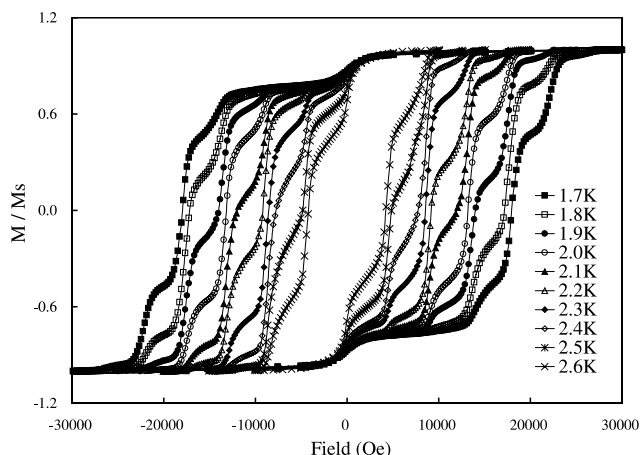


Fig. 2. The plot shows the magnetization hysteresis loops for complex 2 oriented in an eicosane wax matrix at 10 different temperatures.

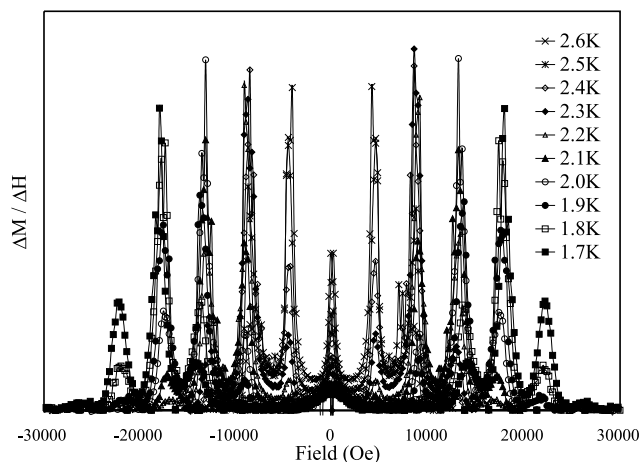


Fig. 3. The plot is shown a plot of the first derivative of magnetization hysteresis loops.

AC magnetic susceptibility studies are an excellent way to detect the slow relaxation of magnetization characteristic of a SMM, which cannot reverse its direction of magnetic moment fast enough to keep in phase with the applied oscillating field while the temperature is lower than its block temperature. The AC susceptibility was obtained for complex 2 in a 1.0 Oe AC field at frequencies (ω) of 250, 500, 750, 1000, 2500, 7500 and 10000 Hz with a DC field of zero. In Fig. 4 are shown the plots of $\chi'_M T$ vs. temperature, where χ' is the real component of the AC magnetic susceptibility. There is a relatively constant value of $\chi'_M T \cong 54 \text{ emu K mol}^{-1}$ in the 10–12.5 K range, and this corresponds to the $\chi'_M T$ value expected for a complex with an $S = 10$ ground state ($g = 1.98$). Also, there are systematic frequency dependence and a “two-step” decrease below 10 K. The decrease in $\chi'_M T$ is attributable to a relaxation process, thus there are two different regions of relaxation; one is the 5.8–8.2 K range and one in the 2.2–3.0 K range.

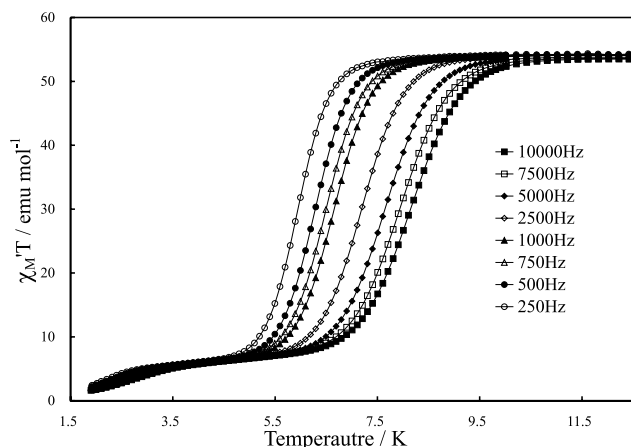


Fig. 4. Plot of $\chi'_M T$ vs. temperature for complex 2 in an AC field of 1.0 Oe oscillating at eight different frequencies.

These two relaxation processes are also shown in Fig. 5, the plots of the out-of-phase χ''_M AC susceptibility vs. temperature, which show predominantly a peak in the 5.8–8.2 K range with a smaller peak in the 2.2–3.0 K range. The lower temperature (2.2–3.0 K) relaxation processes have been interpreted as the defective sites, which four easy axes of complex 1 are forming an angle of 10° with the c -axis in the crystal lattices [24]. However, these two magnetization relaxation processes in Mn_{12} complexes have been elucidated by a Jahn–Teller isomerism [25]. The out-of-phase χ''_M shows a maximum at temperature T_p when $2\pi\omega\tau = 1$. The relaxation time τ is given by $1/\tau = (1/\tau_0) \exp(-U/k_B T)$, where U is the anisotropy energy barrier; τ_0 is the characteristic time of the system. Therefore, by fitting T_p obtained from Fig. 5 for different frequency ω , $\tau_0 = 3.4 \times 10^{-8} \text{ s}$ and $U/k_B = 80.4 \text{ K}$ were obtained for 5.8–8.2 K range, and $\tau_0 = 4.6 \times 10^{-9} \text{ s}$ and $U/k_B = 33.1 \text{ K}$ were obtained for 2.2–3.0 K. The value of anisotropy energy in higher temperature range is larger than that of complex 1 and

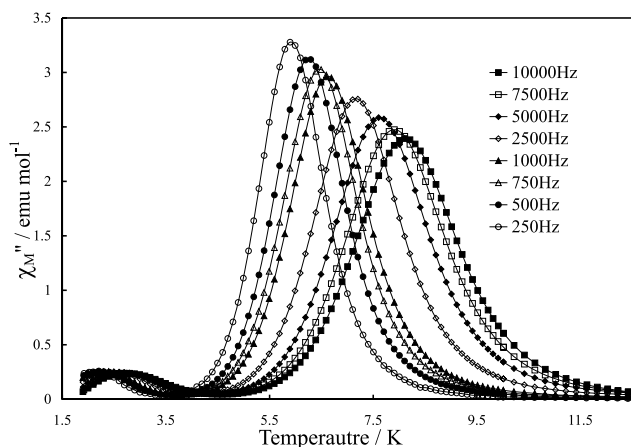


Fig. 5. Plot of χ''_M vs. temperature for complex 2 in an AC field of 1.0 Oe oscillating at eight different frequencies.

the value of anisotropy energy in lower temperature range is smaller than that of complex **1** [24].

From primary results, both frequency dependence in the out-of-phase AC magnetic susceptibilities and steps on hysteresis loops prove complex **2** to be a SMM. The substitution of ligand in the Mn₁₂ system has influenced the anisotropy energies, which would be manipulated by the crystal structure, especially in the molecular packing relative to the *c*-axis. Furthermore, the hysteresis loops on complex **2** will give insight into the mechanism of magnetization tunneling.

Supplementary material

Crystallographic data (excluding structure factors) for complex **2** have been deposited with the Cambridge Crystallographic Data Centre under CCDC 159662.

Acknowledgements

We thank the National Science Council of the Republic of China (NSC-88-2113-M-006-011) for support.

References

- [1] R. Sessoli, D. Gatteschi, A. Caneschi, M.A. Novak, *Nature* 365 (1993) 141.
- [2] L. Thomas, F. Lioni, R. Ballou, D. Gatteschi, R. Sessoli, B. Barbara, *Nature* 383 (1996) 145.
- [3] R. Sessoli, H.-L. Tsai, A.R. Schake, S. Wang, J.B. Vincent, K. Folting, D. Gatteschi, G. Christou, D.N. Hendrickson, *J. Am. Chem. Soc.* 115 (1993) 1804.
- [4] A.R. Schake, H.-L. Tsai, R.J. Webb, K. Folting, G. Christou, D.N. Hendrickson, *Inorg. Chem.* 33 (1994) 6020.
- [5] H.J. Eppley, H.-L. Tsai, N. de Vries, K. Folting, G. Christou, D.N. Hendrickson, *J. Am. Chem. Soc.* 117 (1995) 301.
- [6] S.M.J. Aubin, N.R. Dilley, M. Wemple, M.B. Maple, G. Christou, D.N. Hendrickson, *J. Am. Chem. Soc.* 120 (1998) 839.
- [7] G. Aromi, S.M.J. Aubin, M.A. Bolcar, G. Christou, H.J. Eppley, K. Folting, D.N. Hendrickson, J.C. Huffman, R.C. Squire, H.-L. Tsai, S. Wang, M. Wemple, *Polyhedron* 17 (1998) 3005.
- [8] S.M.J. Aubin, Z. Sun, I.A. Guzei, A.L. Rheingold, G. Christou, D.N. Hendrickson, *Chem. Commun.* (1997) 2339.
- [9] D. Ruiz, Z. Sun, B. Albel, K. Folting, J. Ribas, G. Christou, D.N. Hendrickson, *Angew. Chem. Int. Ed. Engl.* 37 (1998) 300.
- [10] Z. Sun, D. Ruiz, E. Rumberger, C.D. Incarvito, K. Folting, A.L. Rheingold, G. Christou, D.N. Hendrickson, *Inorg. Chem.* 37 (1998) 4758.
- [11] Z. Sun, D. Ruiz, N.R. Dilley, M. Soler, J. Ribas, K. Folting, M.B. Maple, G. Christou, D.N. Hendrickson, *Chem. Commun.* (1999) 1973.
- [12] S.M.J. Aubin, S. Spagna, H.J. Eppley, R.E. Sager, G. Christou, D.N. Hendrickson, *Chem. Commun.* (1998) 803.
- [13] S.M.J. Aubin, Z. Sun, L. Pardi, J. Krzystek, K. Folting, L.-C. Brunel, A.L. Rheingold, G. Christou, D.N. Hendrickson, *Inorg. Chem.* 38 (1999) 5329.
- [14] H.-L. Tsai, T.-Y. Jwo, G.-H. Lee, Y. Wang, *Chem. Lett.* (2000) 346.
- [15] M. Soler, S.K. Chandra, D. Ruiz, E.R. Davidson, D.N. Hendrickson, G. Christou, *Chem. Commun.* (2000) 2417.
- [16] J. An, Z.-D. Chen, J. Bian, J.-T. Chen, S.-X. Wang, S. Gao, G.-X. Xu, *Inorg. Chim. Acta* 299 (2000) 28.
- [17] D. Gatteschi, A. Caneschi, L. Pardi, R. Sessoli, *Science* 265 (1994) 1054.
- [18] J. Villain, F. Hartman-Boutron, R. Sessoli, A. Rettori, *Europhys. Lett.* 27 (1994) 159.
- [19] T. Lis, *Acta Cryst. B* 36 (1980) 2042.
- [20] G.M. Sheldrick, *Acta Crystallogr. A* 46 (1990) 467.
- [21] G.M. Sheldrick, *SHELXL 97* a program for the refinement of crystal structures, University of Göttingen, Germany, 1997.
- [22] J.R. Friedman, M.P. Sarachik, J. Tejada, J. Maciejewski, R. Ziolo, *J. Appl. Phys.* 79 (1996) 6031.
- [23] J.R. Friedman, M.P. Sarachik, J. Tejada, R. Ziolo, *Phys. Rev. Lett.* 76 (1996) 3830.
- [24] W. Wernsdorfer, R. Sessoli, D. Gatteschi, *Europhys. Lett.* 47 (1999) 254.
- [25] S.M.J. Aubin, Z.-M. Sun, H.J. Eppley, E.M. Rumberger, I.A. Guzei, K. Folting, P.K. Gantzel, A.L. Rheingold, G. Christou, D.N. Hendrickson, *Inorg. Chem.* 40 (2001) 2127.